Influence of Preparation Conditions on Network Parameters of Sulfur-Cured Natural Rubber

M. Klüppel,*,† H. Menge,‡ H. Schmidt,§ H. Schneider,‡ and R. H. Schuster†

Deutsches Institut für Kautschuktechnologie e.V., Eupener Strasse 33, D-30519 Hannover, Germany; FG HF-Spektroskopie, Fachbereich Physik, Martin Luther Universität Halle-Wittenberg, D-06099 Halle (Saale), Germany; and Artemis GmbH, Rothwiese 4, D-30559 Hannover, Germany

Received March 20, 2001

ABSTRACT: The effect of initial chain length before cross-linking and sulfur/accelerator amount during curing of natural rubber samples on network parameters (effective chain density, gel fraction, amount of chain ends, entanglement density, trapping factor, and relaxation and correlation times) is investigated by means of proton NMR relaxation, equilibrium swelling, and stress−strain analysis. Remarkable differences are observed in the two sample series depending on the variable initial molar mass. The stress−strain data are evaluated with respect to a non-Gaussian tube model of rubber elasticity that considers the finite extensibility of network chains by referring to the path integral approach of Edwards and Vilgis (*Rep. Prog. Phys.* **1988**, *51*, 243; *Polymer* **1986**, *27*, 483). According to several experimental indications, we assume a nonaffine tube deformation law as first derived by Heinrich et al. (*Adv. Polym. Sci.* **1988**, *85*, 33). The NMR relaxation data are analyzed by considering three types of chains (gel, sol and chain ends). The best fit is obtained by assuming an anisotropic motion of the inter-cross-link chains and chain ends. The swelling data are analyzed by assuming phantom like chains. Within the framework of experimental errors, the network parameters evaluated from the three experimental techniques show fair agreement for both sample series.

1. Introduction

Considerable progress has been obtained in the past in relating the structural parameters of polymer networks to the elasticity properties of rubber vulcanizates.[1−6] This is achieved by considering the various network defects and other deviations of real polymer networks from an ideal network structure. Typical network defects are inelastic, dangling chain ends or closed loop structures. Further deviations from an ideal network structure are due to topological constraints or entanglements of chains that may also be trapped between successive cross-links. The amount of trapped entanglements as well as network defects in general depends on the extent of cross-linking and on the initial molar mass of the polymer before cross-linking.

The classical theory of rubber elasticity is commonly referred to an ideal network structure. It is founded on a random flight statistics of the undeformed chains of a polymer network. In the limit of infinite long chains, it yields a Gaussian distribution function for the end-to-end distance of the network chains. The retracting force of a deformed network is then calculated from the change of the free energy of the chains that results from the deviation of the mean end-to-end distance of the chains from is most probable value. In the classical theory of rubber elasticity, the deformation-dependent part of the free energy of a bulk polymer network is estimated by assuming freely fluctuating, so-called phantom chains that can pass through their neighbors. Topological constraints of a single chain resulting from the surrounding chains (packing effects) are neglected and only cross-link constraints are considered. Though this concept is somewhat unrealistic, it already yields the basic features of rubber elasticity, e.g., the high extensibility of polymer networks and the characteristic temperature dependency of the retracting force that increases with increasing temperature.[1−6]

In a more realistic approach, one has to take into account that real network chains have a finite length and that fluctuations in a bulk polymer network are strongly suppressed due to topological constraints.[1−3] The finite chain length can be considered by referring to the inverse Langevin approach[6,7] or the path integral formulation of a non-Gaussian chain statistics as derived, e.g., by Edwards and Vilgis.[2] Topological constraints acting on the cross-links were considered, e.g., by Kästner[4] or Flory and Erman.[5] This was an important step in explaining the phenomenological C_2 term of the Mooney−Rivlin equation on a molecular level. However, in this first attempt topological constraints were assumed to act on the cross-links alone that were supposed to fluctuate nonisotropically in a strained network, giving rise to an additional deformation-dependent term of the free energy. The application of the path integral formalism of quantum mechanics[8] for a formulation of entropy elasticity by Edwards[2,3,9] allowed us to extend this concept of nonisotropic fluctuations to all chain segments of the network via constraining virtual tubes around the network chains. The deformation of these tubes in a strained network and its effect on the free energy is considered in various tube models of rubber elasticity.[1−3,9]

Solid-state NMR relaxation experiments may provide an advantageous method for the analysis of polymer

* Corresponding author. E-mail: Klueppel@DIKautschuk.de.
† Deutsches Institut für Kautschuktechnologie e.V.
‡ Martin Luther Universität Halle-Wittenberg.
§ Artemis GmbH.

10.1021/ma010490v CCC: $20.00
Published on Web 10/09/2001

network structures. A lot of progress has been made in the field of elastomer characterization using transverse NMR relaxation.[12,36,38] The application of this type of relaxation experiments is based on the high sensitivity of the relaxation process to chain dynamics involving spatial-scale chain motions at temperatures well above the glass transition temperature T_g. Since the polymer chain motion is strongly coupled to the elastomeric structure, chemical information can be obtained by this method in a very sensitive manner. For elastomers well above the glass transition temperature T_g ($T > T_g + 120$ K), the presence of topological constraints and permanent cross-links leads to a nonzero average of the homonuclear and heteronuclear dipolar couplings, which results in a solidlike NMR relaxation behavior.

For polymer networks, this results in typical decays of the transverse NMR magnetization which contains information about network characteristics such as cross-link density and fractions of network chains and defects such as dangling chain ends. This was already shown for a lot of different rubbers.[10−16] Despite a large number of studies dealing with the determination of the total cross-link density in elastomers by NMR methods, there is still a lack of knowledge about the effect of temporary and trapped entanglements on the network density. In the present paper, the NMR results are critically discussed in relation to theoretical approaches and mechanical and swelling investigations. They are compared to the network parameters obtained from the elasticity properties of the bulk networks. These are evaluated by referring to the tube model of Heinrich et al.[1] that is extended according to the approach of Edwards and Vilgis[2] to allow for the consideration of finite chain extensibility. The basic concept of this extended tube model of rubber elasticity is described. Within this framework, we focus on the consideration of trapped entanglements and dangling chain ends. For experimental investigations we refer to a variety of cross-linked natural rubber (NR) samples that differ in cross-linking density and initial molar mass before cross-linking.

2. Theoretical

2.1. The Extended Tube Model of Rubber Elasticity. The path integral formulation of rubber elasticity considers the configurations of chains by space curves $\mathbf{R}(s)$, where s is the arc length of the chains. The local topological constraints acting on the chains in bulk polymer networks are considered by a harmonic potential that forces the chain to remain in a virtual tube around its mean position $\hat{\mathbf{R}}(s)$. The probability distribution of $\mathbf{R}(s)$ relative to the mean position $\hat{\mathbf{R}}(s)$ can be expressed as[1−3]

$$\psi[\mathbf{R}(s), \hat{\mathbf{R}}(s)] = \text{const} \times \exp\left\{-\frac{3}{2l_s}\int_0^L \mathrm{d}s\left(\frac{\partial \mathbf{R}}{\partial s}\right)^2 - \frac{l_s\Omega_o^{\,2}}{6}\int_0^L \mathrm{d}s(\mathbf{R}(s) - \hat{\mathbf{R}}(s))^2\right\} \quad (1)$$

Here, const is a normalization constant, $L = nl_s$ is the contour length of the chain, n is the number of statistical segments of length l_s and Ω_o is a scalar measure of the strength of topological constraints. The random walk behavior of the chains is characterized by the (Gaussian) distribution function that is given by the first term of eq 1, while the second term considers the tube constraints. The constraint parameter Ω_o scales with the inverse cross section of the tube, i.e., $\Omega_o \sim d_o^{-2}$, where d_o is the tube radius (mean fluctuation radius) in the undeformed state. The tube radius is assumed to scale with the mean spacing of successive chain entanglements.

In a strained polymer network fluctuations of chain segments are generally considered to be nonisotropic. This can be taken into account by introducing vectorial tube dimensions, d_μ, in direction of the principal axis of the deformation tensor. By assuming that the constraining potential is diagonal in the main axis system and that the mean configuration $\hat{\mathbf{R}}(s)$ transforms affinely under external deformations, one obtains[1−3]

$$d_\mu \equiv \langle (R_\mu(s) - \lambda_\mu \hat{R}_\mu(s))^2\rangle^{1/2} \quad \mu = 1, 2, 3 \quad (2)$$

where λ_μ is the deformation ratio in direction μ of the main axis system. From eq 1, one now obtains the distribution function of a strained polymer network with nonisotropic fluctuations of chain segments if additionally the chains are assumed to be coupled permanently at joint positions. Such random cross-link points at joint positions $\boldsymbol{R}(s_i) = \boldsymbol{R}(s_i')$ can be considered in the path integral eq 1 by a product of Dirac's δ distribution functions over all cross-links $i = 1, ..., M$. It yields for the probability distribution function of a strained network

$$\psi = \text{const} \times \exp\left\{-\int_o^{\hat{L}} \mathrm{d}s\left(\frac{3}{2l_s}\left(\frac{\partial \mathbf{R}}{\partial \mathbf{s}}\right)^2 + \sum_{\mu=1}^{3}\frac{l_s}{d_\mu^{\,4}}(R_\mu(s) - \lambda_\mu \hat{R}_\mu(s))^2\right)\right\}\prod_{i=1}^{M}\delta(\mathbf{R}(s_i) - \mathbf{R}(s_i')) \quad (3)$$

Note that the integration of eq 3 is performed over the whole network of contour length $\hat{L} = N_c L$, where N_c is the number of network chains. A deformation-dependent distribution function is finally obtained if the lateral tube dimensions d_μ that enter into eq 3 are considered as a function of strain. On length scales larger than the cross-link spacing, the network transforms affinely. Accordingly, one might think that the tubes deform affinely, as well. However, a closer examination of tube deformations has shown that a nonaffine deformation is realized in highly entangled systems:

$$d_\mu = d_o\lambda_\mu^{\,\nu} \quad \mu = 1, 2, 3 \quad (4)$$

The exponent ν takes the value $\nu = 1/2$ and not $\nu = 1$ as in the case of affine deformations. This was first demonstrated by a self-consistent solution of eq 2 with the distribution function eq 3[1,17−20] and later on was predicted also by using scaling arguments.[20,21] The loss of affinity of the tube dimensions in a strained network results from the fact that part of the chains on length scales below the entanglement length are in an equilibrium state that can be referred to the first relaxation process in the Doi−Edwards terminology.[22] Experimental evidence for the nonaffine tube deformation law eq 4 is given by stress−strain measurements performed at swollen rubber samples[23] and neutron scattering of strained rubbers.[24]

By averaging the canonical partition function for a given network topology, i.e., a set of cross-links and mean tube conformations $\hat{\mathbf{R}}(s)$, over all possible topologies the elastic free energy density can be derived from the distribution function of the network eq 3 together with the tube deformation law eq 4. Then, by performing the deformation-dependent thermodynamic average[1−3,17−20] one obtains in the case of highly entangled networks with strong topological constraints ($d_o^2 \ll Ll_s$) the elastic free energy density:[1,17−20]

$$W \equiv W_c + W_e = \frac{G_c}{2}\left(\sum_{\mu=1}^{3}\lambda_\mu^{\,2} - 3\right) + 2G_e\left(\sum_{\mu=1}^{3}\lambda_\mu^{\,-1} - 3\right) \quad (5)$$

Here, G_c is the elastic modulus that corresponds to the cross-link constraints, and G_e is related to the topological tubelike constraints:

$$G_c = A_c \nu_{mech} k_B T \quad (6)$$

$$G_e = \frac{\rho N_A I_s^{\,2} k_B T}{4\sqrt{6} M_s d_o^{\,2}} \quad (7)$$

The quantity ν_{mech} denotes the mechanically effective chain density, A_c is a microstructure factor, ρ is the mass density, N_A is the Avogadro number, M_s is the molar mass of the statistical segments, k_B is the Boltzmann constant, and T is temperature. The microstructure factor A_c considers the fluctuation of cross-links. It equals $A_c = 1$ for total suppression of cross-link fluctuations and $A_c = {}^1/_2$ for freely fluctuating tetrafunctional cross-links (phantom networks). For a given fluctuation radius d_c of the cross-links, it can be expressed by the error function erf (x) as follows[4]

$$A_c = \frac{1}{2} + \frac{1}{\pi^{1/2}}\left(\frac{K_c \exp(-K_c^{\,2})}{\mathrm{erf}(K_c)}\right) \quad (8)$$

with

$$K_c = \sqrt{6}\frac{d_c}{\langle R_c^{\,2}\rangle^{1/2}} \quad (9)$$

$\langle R_c^2\rangle = Ll_s$ is the average end-to-end distance of inter-cross-link chains in the underformed state. For a derivation of eq 8 compare also ref 25.

The tube model considered so far applies for a network structure with monodisperse chains that all contribute to the elasticity properties to an equal amount. For such an ideal network with tetrafunctional cross-links, the mechanically effective chain density ν_{mech} equals twice the density of cross-links μ_c ($\nu_{mech} = 2\,\mu_c = \nu_c$). In the case of nonideal networks, the presence of defects like dangling chain ends, trapped entanglements, closed loop structures and a polydisperse chain length distribution lead to significant deviations of ν_{mech} from its ideal value ν_c, i.e., the inter-cross-link value. In the literature, different estimates have been proposed to account for the defects of real networks.[6,16,19,20,25−30] The effect of dangling chain ends is often considered according to an approach due to Mullins:[26]

$$\nu_{mech} = \nu_c - \frac{\rho N_A}{M_n} \quad (10)$$

It involves the number molecular weight M_n of the polymer chains before cross-linking. The correction term in eq 10 corresponds to the consideration of a gel point $\nu_c^* = 2\mu_c^* = \rho N_A/M_n$ of the network, i.e., the amount of cross-links necessary to connect all initial chains of the un-cross-linked system to a gel.

The additional influence of trapped entanglements on the density of mechanically effective chains was considered in a semiempirical manner by Mullins,[26] as well. By referring to the different fluctuation behavior of cross-links and entanglements, it can be expressed as follows:[25,28]

$$\nu_{mech} = (\nu_c - \nu_c^*) + \frac{A_e}{A_c}\nu_e T_e \quad (10')$$

Here, T_e is the trapping factor of entanglements ($0 < T_e < 1$) that is also termed Langley trapping factor.[27] The quantity ν_e denotes the density of chains between successive entanglements that varies with the inverse of the squared tube radius d_o.

Equation 10′ considers the combined effect of chain ends and trapped entanglements on the mechanically effective chain density. A_e is the microstructure factor of trapped entanglements that considers the fluctuations of trapped entanglements. It can be determined from the fluctuation radius d_o of entanglements similar to the estimation procedure for the cross-links in eqs 8 and 9.[25] Due to the high mobility of trapped entanglements one can conclude that d_o is significantly larger than d_c. Accordingly, the microstructure factor of trapped entanglements can assumed to be well approximated by the value $A_e = {}^1/_2$, which is the limiting value of eq 8 for large fluctuation radii. The microstructure factor A_c is now related to the mean end-to-end distance of all junctions, i.e., cross-links and trapped entanglements. Hence the average $\langle ... \rangle$ in eq 9 has to be performed over both types of chains, which yields $A_c \approx 0.67$, independent of cross-linking density.[25]

The above concept of topological constraints in bulk polymer networks has been developed in the Gaussian limit of infinite long chains. For that reason the finite extensibility of real polymer networks is not considered and no singularity appears in the elastic free energy density eq 5. A singularity can be obtained if, instead of the Gaussian distribution function for the end-to-end distance of network chains, a non-Gaussian chain statistic, e.g., the inverse Langevin approximation, is used.[6,7,23,25,28,29] Following the line of previous papers[19,20,23,25,28] we apply this modification for the cross-link term W_c of eq 5, only, and treat the topological constraint term W_e in the Gaussian limit. This simplification of the model is motivated by recent molecular-statistical investigations of tube like network models based on non-Gaussian network chains, which show that the action of tube constraints becomes weaker in the case of predominance of finite chain extensibility.[2,31,32]

In the framework of the path integral formulation of rubber elasticity, the simplest way to obtain a singularity for the free energy is a modification of the first term of eq 1 as proposed by Edwards and Vilgis[2]

$$\psi[\mathbf{R}(s)] = \text{const} \times \exp\left(-\frac{3}{2l_s}\int_o^L ds\left(\frac{(\mathbf{R}'(s))^2}{1-(\mathbf{R}'(s))^2} + \gamma(\mathbf{R}''(s))^2\right)\right) \quad (11)$$

where $\mathbf{R}'(s) \equiv \partial\boldsymbol{R}(s)/\partial s$ and $\boldsymbol{R}''(s) \equiv \partial^2\boldsymbol{R}(s)/\partial s^2$. A first simplification of eq 11 is obtained by replacing $\boldsymbol{R}'(s)$ in the denominator by its average in a self-consistent manner.[2] Furthermore, the second term of eq 11 with $\boldsymbol{R}''(s)$, ensuring the existence of the path integral, can be omitted if rapid changes on small length scales are smoothened out. This has been shown by Edwards and Vilgis,[2] who restricted the considerations to the level of the primitive path (mean position $\hat{\mathbf{R}}(s)$). They showed that it ensures the existence of the path integral eq 11 by damping the large fluctuation modes with wavenumber $k > k_o$. If the cutoff wavenumber is chosen as $k_o = d_o^{-1}$, then the primitive path is recovered.

Following the argument in ref 32, we chose the cutoff wavelength here in an alternative way

$$k_o = T_e^{1/2}/d_o \quad (12)$$

where T_e is the Langley trapping factor.[27] It produces a modified primitive path between trapped entanglements, only, instead of all entanglements. It means that rapid fluctuations on length scales below the mean spacing of trapped entanglements are smoothened out. Then, the mean value of $(\boldsymbol{R}'(s))^2$ is obtained as[2,32]

$$\langle \mathbf{R}'^2 \rangle \approx (k_o l_s)^2 = \frac{T_e}{n_e} \quad (13)$$

Here, the tube radius d_o is identified with the mean spacing of successive chain entanglements ($d_o = l_s n_e^{1/2}$) and n_e is the mean number of statistical segments between successive entanglements. The elastic free energy is then found from eqs 11−13 with a modified cross-link term of eq 5:[2,32]

$$W = \frac{G_c}{2}\left\{\frac{(\sum_{\mu=1}^{3}\lambda_\mu^2 - 3)\left(1-\frac{T_e}{n_e}\right)}{1-\frac{T_e}{n_e}(\sum_{\mu=1}^{3}\lambda_\mu^2 - 3)} + \ln\left(1-\frac{T_e}{n_e}(\sum_{\mu=1}^{3}\lambda_\mu^2 - 3)\right)\right\} + 2G_e(\sum_{\mu=1}^{3}\lambda_\mu^{-1} - 3) \quad (14)$$

Equation 14 considers the finite chain extensibility of polymer networks together with topological tube constraints in the Gaussian approximation. In the limit $n_e \rightarrow \infty$ the Gaussian formulation of infinite long chains, eq 5, is recovered. The singularity of W is found for $n_e/T_e = \Sigma\lambda_\mu^2 - 3$, where the cross-link term becomes infinite. This corresponds to the situation that the chains between successive trapped entanglements are fully stretched out. This makes clear that the approach in eqs 11−14 characterizes trapped entanglements as some kind of physical cross-links (slip-links) that dominate the extensibility of the network due to the larger number of entanglements as compared to chemical cross-links.

The engineering stress $\sigma_{o,\mu}$ relates the force f_μ in direction μ to the cross section $A_{o,\mu}$ in the undeformed state. It is found from eq 14 by differentiation: $\sigma_{o,\mu} = \partial W/\partial\lambda_\mu$. In the case of uniaxial extension with $\lambda_1 = \lambda$, $\lambda_2 = \lambda_3 = \lambda^{-1/2}$ this yields

$$\sigma_{0,1} = G_c(\lambda - \lambda^{-2})\left\{\frac{1-T_e/n_e}{\left(1-\frac{T_e}{n_e}(\lambda^2 + 2/\lambda - 3)\right)^2} - \frac{T_e/n_e}{1-\frac{T_e}{n_e}(\lambda^2 + 2/\lambda - 3)}\right\} + 2\,G_e(\lambda^{-1/2} - \lambda^{-2}) \quad (15)$$

In the limit of small strains, $\lambda = (1 + \epsilon) \rightarrow 1$ or $\epsilon \rightarrow o$, and by assuming the Gaussian limit $n_e \rightarrow \infty$, one obtains the Young modulus E_o from a Taylor expansion of eq 15:

$$E_o = \lim_{\epsilon\rightarrow 0}\frac{\sigma_{0,1}}{\epsilon} = 3(G_c + G_e) \quad (16)$$

This shows that the Young modulus is strongly influenced by the deformation of the tubes, since the cross-link- and topological constraint term, G_c and G_e, contribute to equal amounts (see below).

2.2. Dipolar Residual Coupling and Proton NMR Relaxation of Network Chains. It is well-known that the decay of the transverse magnetization of nuclear spins, induced by dipolar interactions, is an important source of information about the dynamics of polymer chains in a variety of physical conditions, e.g., in the melt of entangled chains or in molecules cross-linked in a rubber network. The NMR method is sensitive to angular anisotropic segmental motion which is spatially inhibited by chemical cross-links and topological hindrances. The persistence of angular correlations on the time scale set by the residual dipolar interactions and the presence of temporary or permanent constraints (entanglements or cross-links, respectively) leads to a nonexponential decay of the transverse magnetization. The shape of the line broadening ("solidlike effect") visualizes the dynamic influence of these constraints.

The residual part of the dipolar interaction can be described by the scaling concept. It was introduced in 1942 by Kuhn and Grün[7] and was developed straightforward for NMR by Cohen-Addad[33] and Gotlib[34] in the 1970s and Brereton[35] and Sotta and others[36] in the last few years. The starting point is the angular dependence of the dipolar (or quadrupolar) interaction

$$\delta\omega(\vartheta) = \Delta P_2(\cos\vartheta) \quad (17)$$

whereby $\Delta = \mu_0\gamma_H^2 h/(8\pi^2 r^3)$ is the coupling strength. Here, h is the Planck constant, μ_o is the magnetic moment, and γ_H the proton gyromagnetic ratio. $P_2(\cos\vartheta)$ represents the second Legendre polynomial, and ϑ is the angle between the interaction vector r, connecting the two protons, and the static magnetic field B_0. For an isotropic rigid lattice of spin pairs the result is $\langle P_2(\cos\vartheta))^2\rangle = {}^1/_5$,[37] and the second moment $M_2^{rl} = \langle(\delta\omega)^2\rangle$ can be calculated as[13]

$$M_2^{rl} = \frac{9}{4}\Delta^2\,\langle(P_2(\cos\vartheta))^2\rangle = \frac{9}{20}\Delta^2 \quad (18)$$

In the case of a very fast anisotropic motion ($\nu \gg 10^6$ s^{-1}) of a segment vector in the molecular system around the end-to-end vector R, the second moment can be reduced by pre-averaging to the residual second moment M_2^{Res} of a slow and more isotropic motion (motional averaging). It can be written by using the addition theorem of the Legendre polynomials after averaging about the projection angle on the $R-B_0$ plane:

$$M_2^{Res} = \langle[\omega_{Res}(\vartheta)]^2\rangle = \frac{9}{4}\Delta^2\langle\overline{(P_2(\cos\theta))}^2(P_2(\cos\gamma))^2\rangle \tag{19}$$

Here θ is the angle between the interaction vector r and the end-to-end vector R and γ is the angle between R and B_0. The time average $\overline{(P_2(\cos\theta))}$ can be separated from the spatial mean value.

$$M_2^{Res} = \frac{9}{4}\Delta^2\overline{(P^2(\cos\theta))}^2\langle(P_2(\cos\gamma))^2\rangle \tag{20}$$

The preaveraging factor is inversly proportional to the number n of statistical segments—often called the "Kuhn statistical segment"—consisting of about 5−10 backbone bonds[13] and with a factor K depending on the geometry of the molecule. Because of the isotropic state of the network and for a time scale which is long in relation to the segmental motion but short in relation to the motion of the end-to-end-vector, we can use the approximation eq 18 for the averaging of $\langle(P_2(\cos\gamma))^2\rangle$ yielding $^1/_5$ too. The residual second moment of the dipolar interaction (general case) is then

$$M_2^{res} = \frac{9}{4}\Delta^2\left(\frac{K}{n}\right)^2\frac{1}{5} = M_2^{rl}\left(\frac{K}{n}\right)^2 \tag{21}$$

The model used for analysis of the magnetization decays (measured by standard Hahn spin echo sequence) was already described in detail in previous papers.[16,38−41] Hence, we will summarize here only the most important aspects. The rapid anisotropic segmental motion of the network chains described by a number n of freely rotating statistical segments[7,33,36] leads to an nonzero average of the proton dipolar interaction. The decay of the transverse proton NMR magnetization of the network chain is described by

$$\frac{M_N(t)}{M_N(0)} = A\cdot\exp\left\{-\frac{t}{T_2} - M_2^{Res}\tau_s^2\left[\exp\left(-\frac{t}{\tau_s}\right) + \frac{t}{\tau_s} - 1\right]\right\} \tag{22}$$

Here, A is the fraction of network chains in the system, T_2 is the transversal relaxation time related to the fast local motion, and τ_s is the slow relaxation time for large scale rearrangements. It is convenient[34] to introduce a parameter to describe the anisotropy of the rapid motion. This is defined as the ratio $q = M_2^{Res}/M_2^{rl}$. With eq 21, one obtaines for the anisotropy parameter

$$q = M_2^{Res}/M_2^{rl} = (K/n)^2 \tag{23}$$

The factor K, depending on the geometry of the molecule, takes the value $^3/_5$ in the case of a Gaussian chain and a direction of the dipolar interaction vector parallel to the chain. However, we note that the geometry factor in natural rubber (NR) or other elastomers with vinyl or methyl groups is obviously different. In the case of a normal direction of the dipolar interaction vector, like it is usually by C−H bonds of methylen or methyl groups, we must deal with a geometrical factor $K = 3/10$ or 3/20, respectively.[34]

The motion of free sol chains is assumed to be isotropic (liquidlike) and yields to additionally purely exponential decay.[37,38] Then, by assuming an anisotropic motion for the inter-cross-link chains and the dangling free chain ends, the total NMR relaxation is described by[12,16,37−41]

$$\frac{M(t)}{M(0)} = A\exp\left\{-\frac{t}{T_2} - q\cdot M_2^{rl}\tau_s^2\left[\exp\left(-\frac{t}{\tau_s}\right) + \frac{t}{\tau_s} - 1\right]\right\} + B\exp\left\{-\frac{t}{T_2} - q'M_2^{rl}\tau_s\left[\exp\left(-\frac{t}{\tau_s}\right) + \frac{t}{\tau_s} - 1\right]\right\} + C\exp\left\{-\frac{t}{T_{2,sol}}\right\} \tag{24}$$

The fractions A, B, and C represent the parts of magnetization of protons in inter-cross-link chains, dangling ends and sol fraction, respectively. They correspond in a first approximation to the molecular mass parts. qM_2^{rl} represents the mean residual part of the second moment of the dipolar interaction in relation to the physical and chemical constraints. $q'M_2^{rl}$ is the same as before but much smaller ($q' \ll q$) and was introduced by Heuert et al.[16] as a residual part of the second moment due to an assumed anisotropic motion of the dangling chain ends.

By referring to an approach of Scanlan,[29] the fraction A and C of inter-cross-link and sol chains, respectively, can be related to the Langley trapping factor T_e. This concept is based on a counting of elastically effective chains by relating it to the gel fraction and the fraction of chain entanglements that are trapped between two successive cross-links:

$$A = (^3/_2\sqrt{T_e}(1 - C) - T_e/2) \tag{25}$$

The dependency of the trapping factor T_e on the cross-link density is not specified in Scanlan's approach eq 25. However, the value $T_e = 0$ is related to a vanishing fraction of inter-cross-link chains, and $T_e = 1$ refers to the limiting case $A = 1$, where all chains are elastically effective and $B = C = 0$.

Based on Gotlib's idea[34] of the anisotropy parameter $q = M_2^{Res}/M_2^{rl}$, i.e., the ratio between the second moments well above the glass transition temperature and that of the rigid lattice, the average molecular mass of inter-cross-link chains $M_c = n\,M_S$ can be determined. M_S is the molar mass of a statistical segment. Because of the influence of physical entanglements in real networks, the value n that is obtained from eq 23 is not the true inter-cross-link segmental number but an effective one. However, the influence of entanglements is taken into consideration by correcting the value of q by a net value q_0, which is obtained for the un-cross-linked system. It can also be roughly extrapolated from the representation of cross-link density over amount of cross-linker. Then, for the mean molar mass between two cross-links M_c it follows:

$$M_c = \frac{K}{\sqrt{q} - \sqrt{q_0}} M_s \tag{26}$$

It has been demonstrated in earlier papers[13−16,38−41] that this method is a simple and fast tool for network characterization when all experiments are performed at temperatures well above $T_g + 120$ K. Good correlation was obtained between the M_c values estimated from different methods for moderately cross-linked samples with $M_c < 10^4$ g/mol, while agreement between them was poor for loosely cross-linked samples with $M_c > 10^4$ g/mol.[42] Parameters characterizing the network such as M_c, B, T_2, and τ_s showed a tendency similar to that of the swelling and mechanical data.

3. Experimental Section

3.1. Sample Preparation. For experimental investigations, two different series of natural rubber (NR) samples, with high and low molar masses, were mixed on a roller mill and cross-linked at 150 °C up to the maximum torque found in vulcameter curves. The cross-linking was performed with a variable amount of sulfur and *N*-cyclohexylbenzothiazol-2-sulfenamide (CBS) together with 3 phr (per hundred rubber) ZnO and 2 phr stearinic acid. The ratio between CBS and sulfur was kept constant for all prepared samples (CBS/sulfur = 0.18). For the one type of samples with large initial molar mass an untreated NR (RSS #1) was chosen. The second series of samples was prepared with a highly degraded NR (RSS #1) that was obtained by mechanical treatment of the melt for 30 min on a cooled roller mill. The characteristic molar mass was estimated by gel permeation chromatography as $M_n = 249\,000$ g/mol and $M_w = 565\,000$ g/mol in the case of the untreated NR and $M_n = 65\,000$ g/mol and $M_w = 129\,000$ g/mol in the case of the mechanically degraded NR. The polydispersities are given as $M_w/M_n = 2.27$ and 1.98, respectively.

3.2. Mechanical Investigations. Uniaxial stress−strain measurements were performed on (S2) strip-samples with a tensile tester (Zwick 1445) up to rupture stress. The stretching velocity was chosen to be small (10 mm/min) in order to avoid dynamical contributions to the moduli. This corresponds to a strain rate of $\partial\epsilon/\partial t \approx 4 \times 10^{-3}$ s^{-1}. Note that even for this small strain rate the systems are not in full thermodynamic equilibrium. This can be seen if the tensile test is stopped at a certain fixed strain and relaxation of the stress is observed. For a stopover during the up-cycle, the stress decreases somewhat, and for the down-cycle, it increases, indicating that the equilibrium stress lies between the up- and down-cycle data. However, for the case of unfilled rubbers and low strain rates as above, the observed difference between the up and down cycles is small, and the equilibrium stress−strain curve can be well approximated by the up-cycle curve. Furthermore, in view of a minimization of dynamic contributions and to suppress stress-induced crystallization, all measurements were performed in a heating chamber at 100 °C. The Young moduli were measured under the same conditions as above, but with a highly sensitive force transducer in the strain regime up to 5%, only, where the stress−strain curves are almost linear.

Under the above conditions the measured quasi-static stress−strain curves up to rupture are well suited for an experimental test of the tube model based on equilibrium statistical mechanics as considered in the theoretical section 2.1. We note that long time relaxation phenomena of polymer networks, as observed in stress relaxation- and creep experiments, are not completely included in the proposed theory of rubber elasticity. For the discussion of long time relaxation caused by topological constraint release effects compare, e.g., the paper of Heinrich and Vilgis[46] and references therein.

3.3. Proton NMR Relaxation. All experiments were carried out on a Varian Unity 400 widebore spectrometer. The measurement of the transverse relaxation was performed using standard Hahn echo sequence operating at 400 MHz for protons to eliminate the influence of magnetic field inhomogeneities and of chemical shift on the transverse decay, while the dipolar interaction is not affected. All relaxation measurements were performed at $T = 60$ °C, for which the condition $T = T_g + 120$ K (T_g is the glass transition temperature) is fulfilled, approximately. A signal-to-noise ratio of 1000 to 10 000 is necessary to analyze the relaxation curves by using a model with a large number of parameters. A least-squares fit based on Levenberg−Marquardt algorithm was used to approximate the theoretical to the experimental decay.

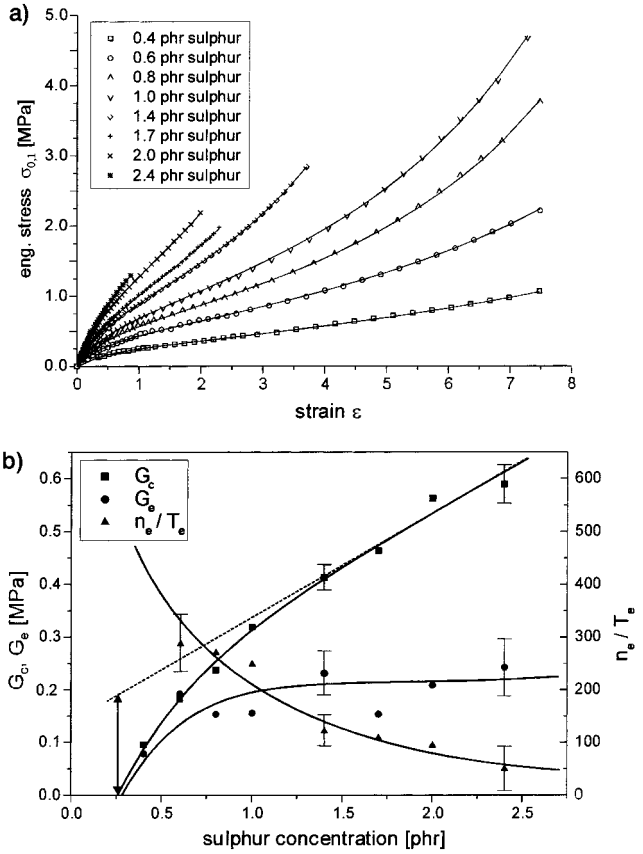

Figure 1. Uniaxial stress-strain analysis of variously cross-linked, untreated NR-networks with high initial molar mass ($M_n = 249\,000$ g/mol). (a) Stress−strain data (symbols) and fittings (solid lines) according to eq 15. (b) Evaluation of fitting parameters with cross-linker concentration. The solid lines serve as guide for the eyes. The dashed line corresponds to eqs 6 and 10′ with $T_e = 1$.

3.4. Equilibrium Swelling. Swelling experiments of the two series of NR-samples were performed at room temperature in toluene up to equilibrium. The effective chain density ν_c(chem) was estimated by assuming phantom like chains and applying the Flory−Rehner equation.[43]

4. Results and Discussion

In view of an experimental test of the proposed models of rubber elasticity and transversal relaxation of polymer networks, the predictions of network parameters from mechanical, NMR relaxation, and equilibrium swelling data are compared. Figures 1a and 2a show uniaxial stress−strain data of the untreated high molar mass NR samples ($M_n = 249\,000$) and the mechanically treated low molar mass NR samples ($M_n = 65\,000$), respectively. The data were obtained for different amounts of cross-linker (sulfur/CBS), as indicated. The solid lines are fitted according to eq 15. The correlation coefficient of the fittings is large in all cases ($R^2 > 0.999$). The development of the three fitting parameters G_c, G_e, and n_e/T_e with increasing amount of cross-linker

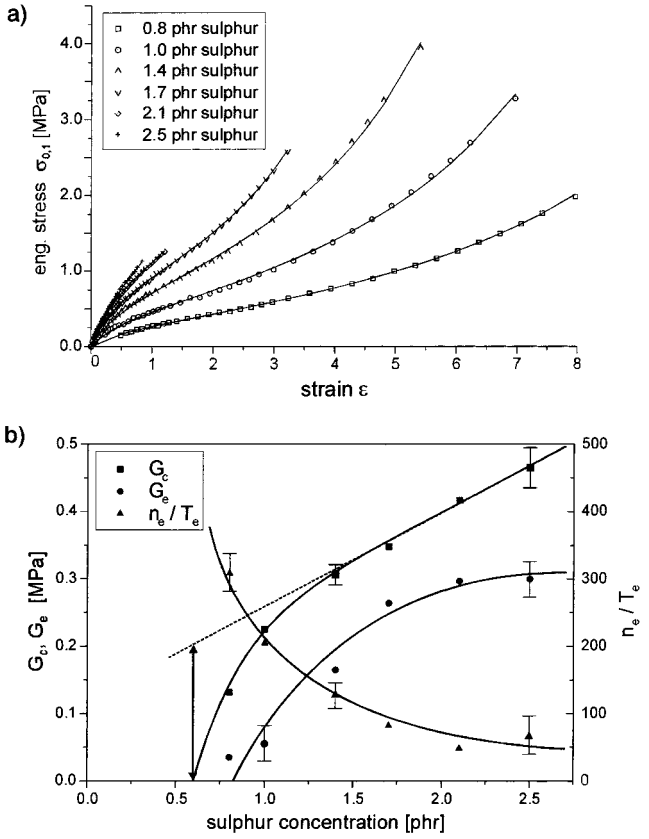

Figure 2. Uniaxial stress−strain analysis of variously cross-linked, mechanically treated NR-networks with low initial molar mass (M_n = 65 000 g/mol). (a) Stress−strain data (symbols) and fittings (solid lines) according to eq 15. (b) Evaluation of fitting parameters with sulfur concentration. The solid lines serve as guide for the eyes. The dashed line corresponds to eqs 6 and 10′ with $T_e = 1$.

is shown in Figures 1b and 2b, respectively. Obviously, starting from a gel point (GP) at cross-linker concentrations of about 0.25 and 0.6 phr, respectively, both moduli G_c and G_e increase while the finite extensibility parameter n_e/T_e decreases. The topological constraint modulus G_e increases first and then approaches a plateau value located between 0.2 and 0.3 MPa in both cases. This plateau value is governed by the constant entanglement density of the rubber. From eq 7 we expect this plateau value to equal almost half of the viscoelastic plateau modulus $G_N^o = {}^4/_5\nu_e k_B T \approx 0.46$ MPa of the NR melt evaluated at 100 °C.[44,45] The obtained plateau value of G_e is in fair agreement with this expectation.

The behavior of the cross-link modulus G_c given by eq 6 can be understood if the form of eq 10′ for ν_{mech} is assumed. Therewith, the maximum entanglement contribution $\nu_e A_e/A_c$ corresponding to $T_e = 1$ can be evaluated if the limiting slope of G_c is extrapolated to the gel point GP (dashed lines of Figures 1b and 2b). The deviations of the experimental G_c data from the limiting dashed lines allow for an estimation of the trapping factors that increase from $T_e = 0$ at the gel points to its limiting values one at high cross-link concentrations.

The results of this evaluation procedure are summarized in Table 1, where beside the values for ν_{mech} and ν_c (here denoted ν_c(mech)), also the trapping factors T_e (here denoted T_e(mech)) are listed. They are compared to the swelling results ν_c(chem) and the NMR results ν_c(NMR) and T_e(NMR), respectively. The inter-cross-link chain density ν_c(NMR) given in Table 1 is evaluated from the M_c values listed in Table 2 by using the equation $\nu_c(\text{NMR}) = A\rho/M_c$ that also involves the fraction A of inter-cross-link chains. Thereby, a mass density of $\rho = 0.9$ g/mol has been used. The trapping factors T_e(NMR) are obtained by referring to Scanlan's[29] approach and the NMR results of the inter-cross-link chain fraction A and the sol fraction C entering eq 25.

Analyzing the data of Table 1, one observes that, irrespective of sample series, the trapping factors T_e(mech) and T_e(NMR), respectively, both increase with increasing sulfur concentration. The two evaluation procedures give roughly the same results, but systematically smaller values are found from the NMR data. A possible reason for this deviation can be the sol fraction C in the samples that is not taken into account in the treatment of the mechanical data. A comparison of the obtained inter-cross-link chain densities shows fair agreement between ν_c(mech), ν_c(chem), and ν_c(NMR), though significant deviations occur in some cases. In particular, this indicates that the swelling equilibrium is mainly governed by the cross-links and entanglement contributions are small (phantom chains). It also confirms the influence of entanglements on the NMR relaxation data as considered in eq 26. In the last two columns of Table 1, the Young modulus E_0, obtained at very small strains below 5%, is compared to the sum $3(G_c + G_e)$, evaluated in the whole strain regime up to

Table 1. Network Parameters from Uniaxial Stress−Strain, Swelling, and NMR Analysis of Sulfur-Cured NR-Networks of Various Cross-Linker Concentrations and Initial Molar Masses[a]

sample	sulfur [phr][b]	ν_{mech} [10^{-5} mol/cm^3]	ν_c(mech) [10^{-5} mol/cm^3]	ν_c(chem) [10^{-5} mol/cm^3]	ν_c(NMR) [10^{-5} mol/cm^3]	T_e(mech)	T_e(NMR)	E_0 [MPa]	$3(G_c + G_e)$ [MPa]
H1	0.4	6.0	1.9	3.7	2.6	0.36	0.24	0.86	0.53
H2	0.6	10.8	3.8	6.6	5.3	0.61	0.43	0.97	1.12
H3	0.8	14.1	6.2	8.8	6.3	0.69	0.52	1.13	1.17
H4	1.0	19.3	9.2	10.5	10.1	0.89	0.63	1.30	1.42
H5	1.4	25.0	13.9	13.8	11.5	0.97	0.70	1.69	1.92
H6	1.7	28.0	17.1	16.2	19.0	0.96	0.84	1.76	1.86
H7	2.0	34.0	21.0	18.3	17.5	1.14	0.84	2.12	2.31
H8	2.4	35.5	25.4	21.0	21.2	0.88	0.87	2.29	2.47
L1	0.8	8.0	1.8	4.5	2.3	0.52	0.41	0.67	0.50
L2	1.0	13.5	3.6	6.8	4.9	0.83	0.51	0.86	0.84
L3	1.4	18.4	7.0	10.3	7.8	0.95	0.64	1.25	1.41
L4	1.7	20.9	9.4	12.8	12.5	0.96	0.75	1.43	1.83
L5	2.1	25.1	12.8	16.0	14.1	1.03	1.15	1.78	2.13
L6	2.5	27.9	16.5	19.1	16.7	0.98	0.80	2.01	2.28

[a] H1−H8: M_n = 249 000 g/mol. L1−L6: M_n = 65 000 g/mol. [b] phr: per hundred rubber.

Table 2. Fitting Parameters Obtained with $K = 3/10$ from the Proton NMR Relaxation Analysis of Sulfur-Cured NR-Networks of Various Cross-Linker Concentrations and Initial Molar Masses[a]

sample	sulfur [phr][b]	T_2 [ms]	T_2^{sol} [ms]	τ_s [ms]	q'/q	A [%]	B [%]	C [%]	qM_2 [(ms)$^{-2}$]	M_c [g/mol]
H1	0.4	12.1	9.7	7.8	0.225	57.6	36.6	5.8	0.402	19 900
H2	0.6	10.6	12.0	3.1	0.245	74.0	23.0	3.0	0.496	12 500
H3	0.8	7.3	12.6	7.2	0.166	79.3	18.0	2.7	0.521	11 400
H4	1.0	8.3	11.8	3.9	0.187	84.4	12.9	2.7	0.692	7500
H5	1.4	4.4	11.3	49.1	0.120	87.1	10.2	2.7	0.748	6800
H6	1.7	5.4	15.2	1.7	0.115	93.0	5.3	1.7	1.112	4400
H7	2.0	3.2	16.1	5.8	0.040	93.1	5.1	1.8	1.025	4800
H8	2.4	2.6	15.8	4.0	0.007	94.1	4.3	1.6	1.234	4000
L1	0.8	5.3	5.1	-	0.21	54.3	23.5	22.2	0.351	21 000
L2	1.0	5.9	5.2	-	0.18	65.5	19.3	15.2	0.457	12 000
L3	1.4	4.1	4.4	-	0.22	71.4	14.7	13.9	0.590	8200
L4	1.7	4.4	4.3	-	0.18	79.0	10.7	10.3	0.798	5700
L5	2.1	2.8	3.8	-	0.02	87.7	2.6	9.7	0.807	5600
L6	2.5	2.3	4.6	-	0.06	87.4	7.6	5.0	0.959	4700

[a] H1−H8: $M_n = 249\,000$ g/mol. L1−L6: $M_n = 65\,000$ g/mol. [b] phr: per hundred rubber.

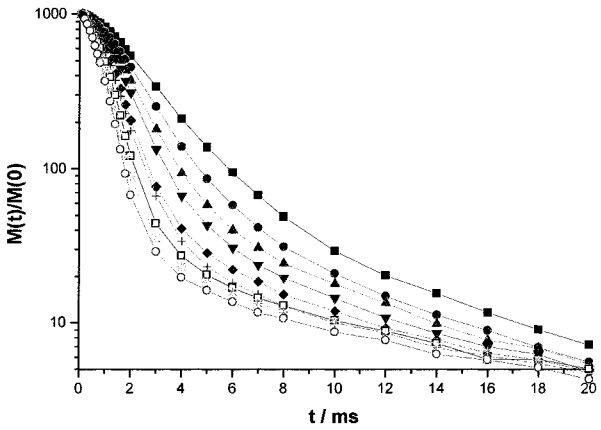

Figure 3. Proton Hahn echo decays for NR-networks with increasing amount of sulfur (S) as cross-linker (from 0.4 phr to 3 phr) prepared from the untreated natural rubber (NR) ($M_n = 249\,000$ g/mol). The ratio between accelerator and sulfur was kept constant at [CBS]/[S] = 0.18 for all samples under study. The transversal magnetization decays were measured at 60 °C and at a proton Larmor frequency of 400 MHz: (■) 0.4 phr S; (●) 0.6 phr S; (▲) 0.8 phr S; (▼) 1.0 phr S; (◆) 1.4 phr S; (+) 1.7 phr S; (□) 2.0 phr S; (∗) 2.4 phr S; (○) 2.7 phr S. The lines serve as a guide for the eyes only.

very large strains (Figures 1a and 2a). It becomes obvious that the prediction of eq 16 is quite well fulfilled, confirming the applied non-Gaussian tube model of rubber elasticity.

In Figure 3, the proton decays of transversal magnetization obtained by a Hahn-spin echo pulse sequence are plotted for static samples under investigation at 60 °C (approximately $T_g + 120$ K). The smallest echo time in this experiments was 80 μs and this leads to a partial loss of a few data points (up to four data points under current experimental conditions) in the initial part of the decay governed by the proton−proton dipolar coupling. However, no magnetization decay can be fitted by a single relaxation decay. For analyzing the decays we have applied a relaxation function which is widely and successfully exploited in rubbery materials. This function takes the form of eq 24, where A, B, and C correspond to the fractions of the Gauss-like relaxation (arising from the inter-cross-linked chains and dangling chain ends) and one pure exponential (liquidlike) fraction due to free chains.

By using this function, eq 24, the magnetization decays in Figure 3 are well fitted in each case for the sample series H without previous mechanical treatment on a laboratory mill ($M_n = 249\,000$). For the sample series L with mechanical treatment before cross-linking ($M_n = 65\,000$) the τ_s was assumed to be static during the experimental window to get a better fit. All NMR fitting parameters are summarized in Table 2. The M_c values are evaluated from eq 26 by assuming a segmental mass of the NR chains $M_s = 85$ g/mol.[44,45] The residual parts of the magnetic moment due to an anisotropic motion of the un-cross-linked rubbers were measured as $q_oM_2 = 0.27$ (ms)$^{-2}$ for the sample series H and $q_oM_2 = 0.23$ (ms)$^{-2}$ for the series L, respectively. The anisotropy parameters are then evaluated with the van Vleck second moment $M_2(\mathrm{NR}) = 0.86 \times 10^4$ (ms)$^{-2}$.[13,16,39]

As shown in Figure 4 the decays of the transversal magnetization for the samples of low and high initial molar masses (with and without mechanical treatment) with the same amount of sulfur/CBS are very similar up to 2 ms echo time, but show a different long time behavior due to differences in the relaxation times. These differences are even more pronounced in the un-cross-linked samples. The magnetization of the untreated rubber is decaying much more slowly at longer echo times, and the Gaussian-like shape at the beginning is more clearly visible. There is no significant difference in the residual second moment q_oM_2 of the both un-cross-linked samples (see above). However, the fractions of hindered, entangled chains A and dangling chain ends B are changing with the duration of the mechanical treatment (30 min). Fraction A is decreasing and fraction B is increasing in agreement with the observed reduction of the precursor chain length. The relaxation time T_2 decreases a little bit for the low molecular weight, milled rubber.

On the contrary, important differences may be observed comparing cross-linked networks with increasing amount of the cross-linking agent (Table 2). The residual second moment qM_2 is raising with the sulfur/CBS content resulting in higher cross-link density or a smaller mean molecular mass between two knots M_c (eq 26). As fraction A of the inter-cross-linked chains increases, fraction B of the dangling ends is decreasing. For the networks with the high initial molar mass the relaxation time T_2 is decreasing from 12 to 2.6 ms with the cross-linker from 0.4 to 2.4 phr sulfur. The relaxation time T_2^{sol} and the fraction C of the free chains show a relatively constant behavior, the corresponding parameters are on the order of 13 ms and 3%. The

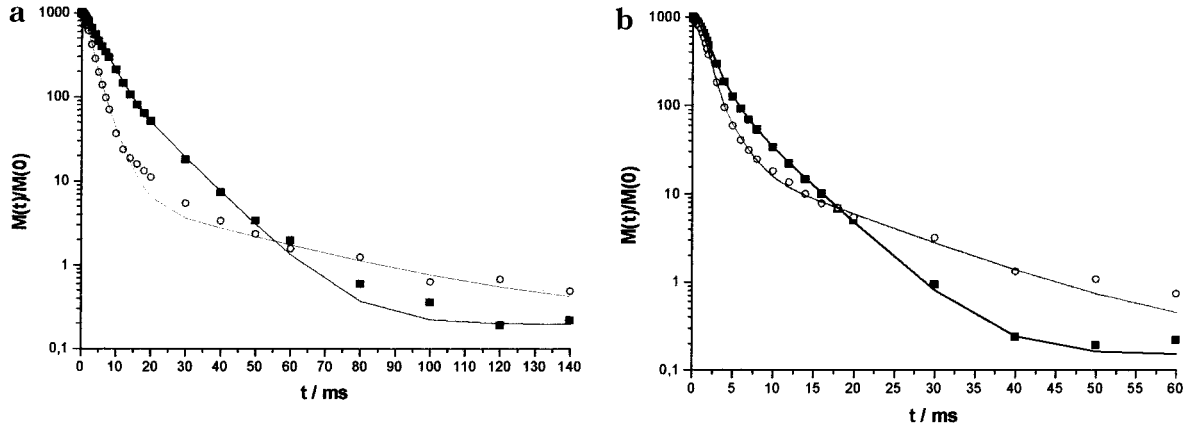

Figure 4. Comparison of the corresponding samples before (M_n = 249 000 g/mol) and after mechanical treatment (M_n = 65 000 g/mol): (a) un-cross-linked NR samples; (b) cross-linked NR networks with 0.8 phr sulfur (S) and [CBS]/[S] = 0.18 prepared from NR with (○) M_n = 249 000 g/mol and (■) M_n = 65 000 g/mol, respectively. The lines are fitted curves from the model (eq 24).

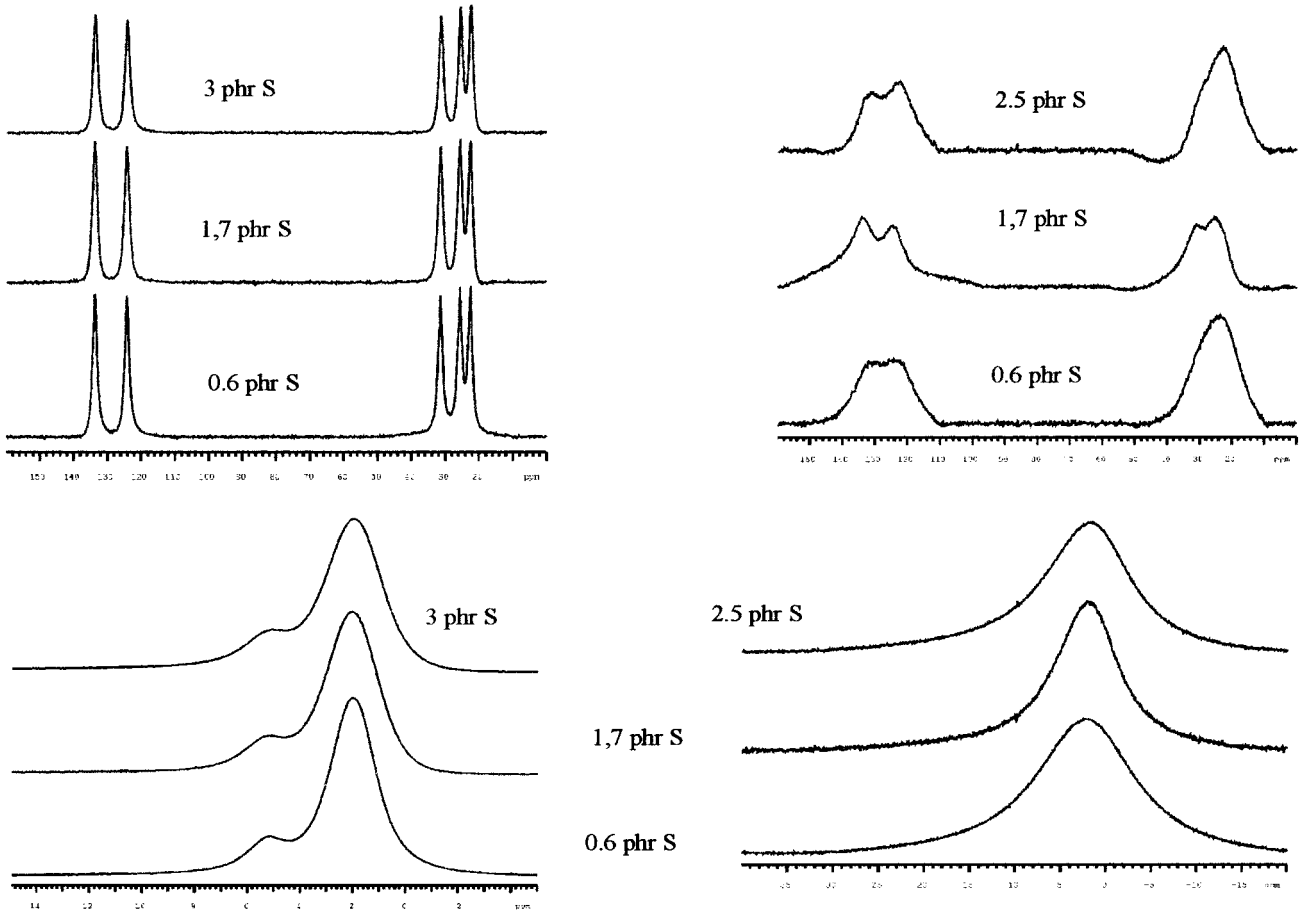

Figure 5. Static ^{13}C (top) and ^{1}H (bottom) spectra of the networks with different amount of cross-linker (0.6, 1.7, and 3 or 2.5 phr S, respectively) for the two networks series prepared from NR with M_n = 249 000 g/mol (left) and M_n = 65 000 g/mol (right), respectively.

values of τ_s show no clear trend, but in contrast to the networks built from the treated rubber, this parameter is needed to get a qualitatively good fit, which indicates a better overall mobility over the whole range. The parameter q'/q is observed to be going down with the amount of cross-linker. That means an anisotropy of the dangling ends is less important at higher cross-link densities.

The networks built from the rubber with the low initial molar mass show the same general trends (Table 2). The main differences are observed in the behavior of the fraction C, which is much larger and decreasing from 22% down to 5%. The relaxation time T_2^{sol} is smaller by a factor of 2−3 (about 5 ms) than that for the corresponding untreated networks and more or less constant. Additionally, the relaxation time T_2 decreases from about 6 to 2 ms, but again this is smaller than for the untreated samples. The smaller relaxation times of these components indicate the dramatic changes in the line width of the static proton and carbon spectra shown in Figure 5. The fraction of the dangling ends B, however, is a little bit larger compared to the untreated networks, the fraction A of inter-cross-linked chains is smaller. The same is valid for the parameter qM_2,

resulting in less cross-linked networks (higher M_c values) by using the same amount of cross-linking agent. This is in good agreement with the results from the mechanical analysis.

5. Conclusions

It has been shown that the initial chain length before cross-linking and the sulfur/accelerator amount have a pronounced effect on the quasi-static mechanical properties and the chain dynamics of natural rubber samples. The network parameters evaluated from three different experimental techniques, uniaxial stress−strain, swelling, and NMR analysis, show fair agreement for the investigated sample series. In particular:

(i) The density of inter-cross-link chains ν_c is found to increase almost linear with the amount of sulfur if a critical concentration, referring to the gel point, is exceeded (Table 1). The T_2 time decreases with rising cross-linking density and is generally smaller for the mechanically degraded systems (Table 2).

(ii) For the mechanically degraded samples with low initial chain length the gel point is shifted to higher sulfur concentrations (≈0.6 phr) as compared to the untreated samples (≈0.25 phr) (Figures 1 and 2).

(iii) The cross-link efficiency (number of cross-links formed per unit of sulfur) is somewhat reduced for the mechanically degraded systems (slope of the dashed lines in Figures 1 and 2). In agreement with this, the amount of inter-cross-link chains A increases less rapidly with sulfur amount for the mechanically degraded samples and the fraction of free chains C is generally larger (Table 2).

(iv) The trapping factor of entanglements T_e increases successively with the amount of sulfur. It shows a weak dependency on initial chain length, only. For moderate sulfur amounts just above the gel point, it increases somewhat faster for the mechanically degraded systems (Table 1).

(v) The proposed tube model with nonaffine tube deformations allows for a reasonable description of quasi-static stress−strain data up to large strains. The predicted dependency of the Young modulus (eq 16) on cross-link and entanglement density is confirmed by the experimental data (Table 1).

Acknowledgment. Helpful discussions with Prof. E. Straube (University of Halle/Wittenberg), Dr. G. Heinrich (Continental AG) and Prof. Th. Vilgis (Max-Planck-Institute, Mainz, Germany) are gratefully acknowledged.

References and Notes

(1) Heinrich, G.; Straube, E.; Helmis, G. *Adv. Polym. Sci.* **1988**, *85*, 33.
(2) Edwards, S. F.; Vilgis, T. A. *Rep. Prog. Phys.* **1988**, *51*, 243; *Polymer* **1986**, *27*, 483.
(3) Deam, R. T.; Edwards, S. F. *Philos. Trans. R. Soc.* **1976**, *A 280*, 317.
(4) Kästner, S. *Faserforsch., Textiltechnik* **1976**, *27*, 1; *Colloid Polym. Sci.* **1981**, *259*, 499, 508.
(5) Flory, P. J. *J. Chem. Phys.* **1977**, *66*, 5720; *Polym. J.* **1985**, *17*, 1. Erman, B.; Flory, P. J. *J. Chem. Phys.* **1978**, *68*, 5363. Flory, P. J.; Erman, B. *Macromolecules* **1982**, *15*, 800, 806.
(6) Treloar, L. R. G. *The Physics of Rubber Elasticity*, Clarendon Press: Oxford, England, 1975.
(7) Kuhn, W.; Grün, F. *Kolloid Z. Z. Polym.* **1942**, *101*, 248.
(8) Feynman, R. P.; Hibbs, A. P. *Quantum Mechanics and Path Integrals*; McGraw-Hill: New York, 1965.
(9) Edwards, S. F. *Proc. Phys. Soc.* **1965**, *85*, 613; **1967**, *92*, 9.
(10) Simon, G.; Birnstiel, A.; Schimmel, K. H. *Polym. Bull.* **1989**, *21*, 235.
(11) Simon, G.; et al. *Polym. Bull.* **1989**, *21*, 475.
(12) Gronski, W.; et al. *Rubber Chem. Technol.* **1992**, *65*, 63.
(13) Simon, G.; Schneider, H. *Makromol. Chem., Macromol. Symp.* **1991**, *52*, 233.
(14) Lee, S.; Pawlowski, H.; Coran, A. Y. *Rubber Chem. Technol.* **1994**, *67*, 854.
(15) Menge, H.; Hotopf, S.; Pönitzsch, St.; Richter, S.; Arndt, K.-F.; Schneider, H.; Heuert, U. *Polymer* **1999**, *40*, 5303.
(16) Heuert, U.; Knörgen, M.; Menge, H.; Scheler, G.; Schneider, H. *Polym. Bull.* **1996**, *37*, 489.
(17) Heinrich, G.; Straube, E. *Acta Polym.* **1984**, *35*, 115.
(18) Heinrich, G.; Straube, E. *Polym. Bull.* **1987**, *17*, 247.
(19) Heinrich, G.; Kaliske, M. *Comput. Theor. Polym. Sci.* **1997**, *7*, 227.
(20) Kaliske, M.; Heinrich, G. *Rubber Chem. Technol.* **1999**, *72*, 602.
(21) Rubinstein, M.; Panyukow, S. *Macromolecules* **1997**, *30*, 8036.
(22) Doi, M.; Edwards, S. F. *J Chem. Soc., Faraday Trans. 2* **1978**, *74*, 1789, 1802, 1818; **1979**, *75*, 38.
(23) Klüppel, M. *Macromolecules* **1994**, *27*, 7179.
(24) Straube, E.; Urban, V.; Pyckhout-Hintzen, W.; Richter, D.; Glinka, C. W. *Phys. Rev. Lett.* **1995**, *74*, 4464.
(25) Klüppel, M.; Heinrich, G. *Macromolecules* **1994**, *27*, 3569.
(26) Mullins, L. *J. Appl. Polym. Sci.* **1956**, *2*, 1.
(27) Langley, N. R. *Macromolecules* **1968**, *1*, 348.
(28) Klüppel, M. *Prog. Colloid Polym. Sci.* **1992**, *90*, 137; *J. Appl. Polym. Sci.* **1993**, *48*, 1137.
(29) Scanlan, J. *J. Polym. Sci.* **1960**, *43*, 501.
(30) Heinrich, G.; Beckert, W. *Prog. Colloid Polym. Sci.* **1992**, *90*, 47.
(31) Kovac, J.; Crabb, C. C. *Macromolecules* **1982**, *15*, 537.
(32) Klüppel, M.; Schramm, J. *Macromol. Theory Simul.* **2000**, *9*, 742.
(33) Cohen-Addad, J. P. *J. Chem. Phys.*, **1974**, *60*, 2440.
(34) Gotlib, Yu. Ya.; et al. *Vysokomol. Soedin.* **1976**, *A 28*, 10, 2299.
(35) Brereton, M. G. *Macromolecules* **1989**, *22*, 3667.
(36) Sotta, P.; Fülber, C.; Demco, D. E.; Blümich, B.; Spiess, H. W. *Macromolecules* **1996**, *29*, 6222.
(37) Abragam, A. *The Principles of Nuclear Magnetism*, Clarendon Press: Oxford, England, 1981.
(38) Simon, G.; Gronski, W.; Baumann, K. *Macromolecules* **1992**, *25*, 3624 and references therein.
(39) Kuhn, W.; Barth, P.; Hafner, S.; Simon, G.; Schneider, H. *Macromolecules* **1994**, *27*, 5773.
(40) Menge, H.; Hotopf, S.; Schneider, H. *Kautsch. Gummi Kunstst.* **1997**, *50*, 268.
(41) Knörgen, M.; Heuert, U.; Menge, H.; Schneider, H. *Angew. Makromol. Chem.* **1998,** *261/262*, 123.
(42) Sakano, H.; Ikawa, K.; Kojima, H. *Kobunshi Ronbunshu* **1997**, *54*, 757.
(43) Flory, P. J.; Rehner, J. *J. Chem. Phys.* **1943**, *11*, 521.
(44) Fetters, L. J.; Lohse, D. J.; Richter, D.; Witten, T. A.; Zirkel, A. *Macromolecules* **1994**, *27*, 4639.
(45) Aharoni, S. M. *Macromolecules* **1983**, *16*, 1722; **1986**, *19*, 426.
(46) Heinrich, G.; Vilgis, T. A. *Macromolecules* **1992**, *25*, 404.

MA010490V